Electron-spin-lattice relaxation in Yb^{3+}-doped silicate glass

S. B. Stevens* and H. J. Stapleton
Department of Physics, University of Illinois at Urbana-Champaign, 1110 W. Green St., Urbana, Illinois 61801
(Received 12 June 1990)

Relaxation rates of Yb^{3+} ions incorporated in low concentrations into a host silicate glass have been measured using a pulse saturation and recovery technique at 9.5 GHz over the temperature range 1.5–7.0 K. Compared with similar measurements made on crystalline material, the temperature dependence of the recovery rates for the two-phonon Raman process is anomalously weak (T^6 instead of T^9). This anomaly suggests the need to modify the Debye density of states. Fractal models have been suggested for the thermal properties of glasses and for similarly anomalous spin-relaxation behavior in proteins. This model is discussed as well as other models of phonon localization in glasses. An estimate for the localization frequency or crossover frequency between extended and localized phonon regimes can be extracted from fits of the data from the sample with the lowest Yb concentration.

I. INTRODUCTION

The nature of the vibrational density of states in disordered solids is an open question and the subject of ongoing research. Even in vitreous silica, which has been investigated extensively, a microscopic description of the phonon density of states is ambiguous. This paper describes the results of electron spin-lattice relaxation measurements on a series of Yb-doped silicate glasses. Because the relaxation rates depend on the phonon density of states in the glass, at low concentrations the Yb spins can be used as a probe. Similar measurements made on protein single crystals[1] and frozen protein solutions[2–10] have shown deviations from the expected temperature dependence of the Raman relaxation rates of a Debye-like solid. Protein relaxation results led to the suggestion of a fractal model[3,11–17] of protein dynamics that is no longer considered viable by most investigators. It was the purpose of this investigation to determine if similar Raman relaxation rate anomalies occur in glasses.

Our samples were provided by M. J. Weber of the Lawrence Livermore Laboratory, where they were previously used in a study of stimulated emission cross sections.[18] Each sample had the host glass composition: 75 mol % SiO_2, 15 mol % Na_2O, 5 mol % BaO, 5 mol % ZnO. Yb_2O_3 was substituted for SiO_2 in five molar concentrations: 0.05, 0.5, 1.0, 2.0, and 4.0 mol %. The coordination of Yb^{3+} in phosphate, silicate, and germanate glasses was studied by Robinson and Fournier.[19] In their silicate glass, similar to ours in composition, they found that the SiO_4 tetrahedra cluster around the Yb^{3+} producing approximately octahedral symmetry at the Yb^{3+} site. This leads to a splitting of the lowest, $J=\frac{7}{2}$, level into four Kramer doublets with the ground doublet about 330 cm^{-1} below the first excited state, thereby eliminating Orbach (resonant Raman) relaxation mechanisms. Optical spectra of the Yb^{3+} ions are given in Ref. 19. There is sufficient variation among Yb^{3+} sites to render the microwave absorption spectrum featureless. As shown in Fig. 1, it is a broad, asymmetric absorption line peaked at 0.23 T, corresponding to a g factor of 2.97. All pulse-saturation and recovery measurements were made at the absorption peak. Under our experimental conditions ($h\nu \ll 2k_BT$) the temperature dependence of the direct relaxation process is approximately linear:

$$\left[\frac{1}{T_1}\right]_{\text{direct}} = R_0 \coth\left[\frac{h\nu}{2k_BT}\right] \approx R_0\left[\frac{2k_BT}{h\nu}\right]. \quad (1)$$

The rate for the two-phonon Raman-scattering process involves an integration over all phonon frequencies. The result for a Kramers ion is given by

$$\left[\frac{1}{T_1}\right]_{\text{Raman}} \propto \int_0^{\nu_{\max}} \frac{\rho^2\nu^4 \exp\left[\frac{h\nu}{kT}\right]}{\left[\exp\left[\frac{h\nu}{kT}\right]-1\right]^2} d\nu . \quad (2)$$

For a spectral dimension m, defined by a phonon density

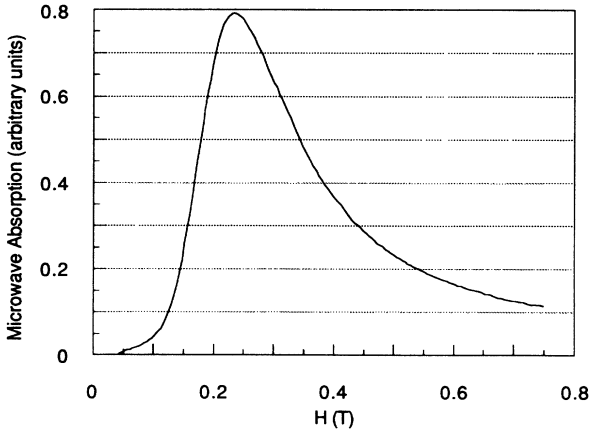

FIG. 1. Absorption spectrum for 0.05-mol % Yb–doped silicate glass obtained at a microwave frequency of 9.5 GHz and a temperature of 1.5 K.

of states,

$$\rho(\nu) \propto \nu^{m-1} , \tag{3}$$

Eq. (2) becomes

$$\left[\frac{1}{T_1}\right]_{\text{Raman}} = CT^{3+2m}\int_0^{x_{\max}} \frac{x^{2+2m}\exp(x)}{[\exp(x)-1]^2}dx$$
$$= CT^{3+2m}J_{2+2m}\left[\frac{\Theta}{T}\right] , \tag{4}$$

where $x = h\nu/kT$ and $x_{\max} = \Theta/T$.

The Debye model requires that $m=3$ and results in the well-known T^9 Raman relaxation rate for Kramers' ions when the Debye temperature $\Theta = h\nu_{\max}/k$ is large compared to T. The T^9 dependence, verified in crystalline materials, has not been observed for paramagnetic proteins, either crystalline or as frozen solutions. In such systems the temperature dependence of the two-phonon relaxation mechanism varies more slowly, roughly as the fifth or sixth power of T. Over small temperature regions, a reduced power-law dependence could be attributed to a low Debye temperature, but measurements on the samples of the copper protein plastocyanin,[8] for example, between 1.4 and 15.6 K require m values between 1 and 1.2 and Debye temperatures of approximately 100 K when the data are fit to Eq. (4).

Because the Debye temperature is such an important parameter in the description of the phonon spectrum of a solid, it is important to have an estimate of its magnitude for a similar glass. The Debye temperature for vitreous silica has been measured from elastic constants[20] and from the Debye-Waller factor in inelastic neutron scattering.[21] The value obtained from elastic measurements depends on the choice of vibrational unit in the solid. If the calculation is made per ion, $\Theta_D = 495$ K. If the vibrational unit is taken to be a SiO_4 tetrahedron, $\Theta_D = 312$ K. When the calculation is made per ion, vibrations between atoms in a SiO_4 tetrahedron are included (optic modes) that are missing in the second value, giving a lower cutoff. Neutron-scattering experiments yield a value of 370 K. For our temperature range (1.5–7 K), the T^9 temperature dependence should hold if Θ_D is taken as the upper cutoff.

We refer to the model described above, Eq. (4) with noninteger m values less than three, as a generalized Debye model to distinguish it from a true fractal model proposed and refined in a series of papers by Orbach *et al.*[11–17] In that model, the quantized vibrational excitations of a fractal lattice (fractons) are localized and lead to a more complicated power-law expression for the Raman (two-fracton) relaxation mechanism. The one- and two-fracton mechanisms are direct analogues of the one- and two-phonon mechanisms for the case of a solid that exhibits fractal vibrational excitations. At very long-length scales all materials will behave as Euclidean structures. It is only for short-length scales that one can expect to see evidence of fractal vibrational excitations. The crossover between these two regimes occurs at a length scale ξ such that $\xi = \lambda$, where λ is the phonon wavelength. This corresponds to a crossover frequency $\nu_c = v/\xi$ where v is the sound velocity. In the Euclidean regime, the Debye approximation is expected to apply for acoustic phonons: $\rho(\nu) \propto \nu^2$ with a linear dispersion relation. In the fractal regime $\rho(\nu) \propto \nu^{m-1}$ and the dispersion relation acquires an imaginary part.

In Ref. 16 the time dependence of the recovery profiles and the temperature dependence of the two-fracton relaxation process are discussed. It is found that in the presence of rapid electronic cross-relaxation the time profile is exponential, with an average relaxation rate

$$(1/T_1)_{\text{av}} \propto T^{2m[1+2(d_\phi/D)]-1} , \tag{5}$$

where m is the spectral dimension, defined by Eq. (3), D is the mass fractal or Hausdorff dimension, and d_ϕ is a dimension that describes the range dependence of the fracton wave function. D is defined by the relation $M_R \propto R^D$, where M_R is the mass within an imaginary sphere of radius R. Since the mass density of amorphous silica is comparable to that of crystalline silica, we would expect D to deviate very little, if at all, from the Euclidean dimension of three. If m, d_ϕ, and D are all variable parameters, any data set displaying a power-law dependence on temperature could be fit by this model with a suitable choice of parameters.

A brief discussion of the experimental apparatus and the steps taken to ensure good thermal contact between the samples and the bath are presented in Sec. II. The results of the measurements are presented in Sec. III. In the lowest-concentration sample, the direct process is found to dominate the relaxation to a temperature of roughly 3 K, where the Raman process rapidly becomes dominant. Fits of the glass relaxation data in the Raman region to various models are presented in Sec. III. In the higher-concentration samples, the direct and Raman processes are still expected to occur, but it was necessary to add a concentration dependent term to the overall expression for the rate in order to fit the data. An analysis of these results will also be presented in Sec. III.

II. EXPERIMENTAL PROCEDURE

The relaxation rates are measured at microwave frequencies near 9.5 GHz using a custom-built, superheterodyne pulse spectrometer. The frequency of the signal klystron (Varian VA153) is locked to a tunable external cavity using a Pound stabilization circuit[22] and a Micro Now model 210 cavity stabilizer. No frequency stabilization is required for the local oscillator (also a Varian VA153). Pulses of microwave power are generated with a Microdynamics MD-20X30D microwave diode switch, shunted by two 15-dB cross guide couplers, a 75-dB variable attenuator, and a phase shifter. The recovery amplitude is monitored with power through the shunt arm following a saturating pulse. The pulse power level, monitor power level, and pulse duration are all adjustable. The recovery signal is digitized and recorded with a LeCroy 2256 signal averager. Through the use of pretrigger sampling we can determine the equilibrium baseline signal, independent of the dwell time of the signal averager.

In the normal mode of operation, the glass sample is

placed in the bottom of a rectangular TE_{101} cavity that is insulated from direct contact with the helium bath by a surrounding copper can filled with ^4He exchange gas. Temperatures are measured and controlled to within ± 4 mK using the output from a bridge circuit that incorporates a calibrated germanium resistance thermometer, which is mounted directly to the upper half of the copper sample cavity. The bridge is part of a temperature control loop utilizing a Linear Research LR-130 temperature controller.

The samples were cut with a Buehler diamond wafering blade. The thinnest slices were ≈ 0.01 cm thick. The samples were cut in thin slabs for two reasons: first, to minimize the thermal path of phonons to the copper-glass interface, and second, to minimize dielectric heating. Samples were attached to the copper cavity bottom with a thin layer of Apiezon N grease. The thermal boundary resistance of such interfaces has been discussed by Anderson.[23]

For the lowest concentrations, the signal-to-noise ratio was increased by attaching additional pieces of the glass to the vertical walls of the cavity. Glass with a molar concentration of 0.001 mol % Yb_2O_3 was also available, but failed to provide sufficient signal-to-noise ratio for these measurements.

Because sample heating in these samples was suspected, measurements were also made in a different probe in which the sample was in direct contact with the liquid-helium bath. In this mode of operation, the measurements were restricted to temperatures below the λ point (2.1 K). Even with the sample immersed directly in liquid helium, the recovery profiles showed some dependence on pulse duration and sample thickness, indicative of sample heating. These results will be discussed in Sec. III.

Under certain experimental conditions, the recovery profiles are not strictly exponential. This appears as a slowing of the recovery rates near equilibrium. This feature of the recovery profile would have made it difficult to determine a baseline were it not for the fact that the equilibrium EPR signal was sampled prior to the saturating pulse. Further advancement of the averaging channel was halted during the saturating pulse. For nearly exponential recoveries, the recovery rate was determined by making a linear regression fit to the logarithm of the recovery amplitude. For extremely nonexponential recoveries, the relaxation can be followed over several orders of magnitude in time by digitizing the same baseline for a number of different dwell times and concatenating the files.

III. RESULTS AND DISCUSSION

A. Characterization of recovery profiles

In order to characterize the spin-lattice relaxation rate as a function of temperature alone, it is necessary to reach a regime where the measured rates are independent of other experimental parameters such as pulse duration and sample thickness. Stretched exponential functions have been used to characterize the recovery profiles in an Yb-doped phosphate glass.[24] Our most consistent data were obtained under the conditions that minimize sample heating: thin samples and short pulses. A dependence of the relaxation rate on sample thickness was most pronounced for the higher-concentration samples. Some thickness dependence in the lower-concentration samples was observed, mostly at the lower temperatures where the direct relaxation mechanism dominates, but the variation in the rates with sample thickness was small compared to the variation with concentration. The main results can be summarized as follows: (i) Recoveries were slower for longer pulse durations, (ii) recoveries were slower for thicker samples, and (iii) pulse duration and sample thickness dependencies were more pronounced for higher concentrations.

Our most reliable data were obtained for the lowest (0.05 mol %) concentration sample. For all other concentrations, the data sets chosen for the most extensive analysis were those measured on thin samples using short pulses. Even for the 0.05-mol % sample, the recovery profiles below 3 K show some dependence on pulse duration and sample thickness. At those temperatures the direct relaxation process is expected to dominate, and the behavior in this region is consistent with a phonon bottleneck. At 4 K, the recoveries in the lowest-concentration sample were nearly pulse duration independent. Recovery profiles illustrating these points are shown in Figs. 2 and 3.

Figure 2 shows a log-log plot of four decay profiles of the 0.05-mol %–doped glass at 1.5 K. The recoveries with 1, 10, and 100 ms pulse durations were measured with the sample in direct contact with the helium bath, and the temperature was controlled by a manostat. The

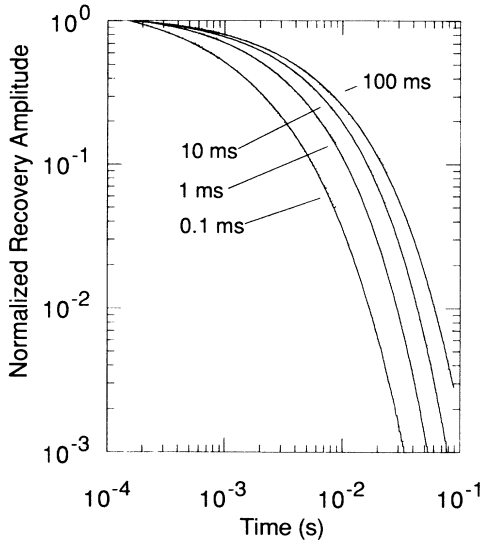

FIG. 2. Recovery profiles for the 0.05-mol %–doped glass at 1.5 K with pulse durations as noted. Recovery profiles with 1, 10, and 100-ms pulse durations were measured with the sample in direct contact with liquid helium. The profile with 0.1-ms pulse durations was measured with the sample isolated from contact with the helium bath. The fits were made to a stretched exponential [Eq. (6)] using the fitting parameters listed in Table I.

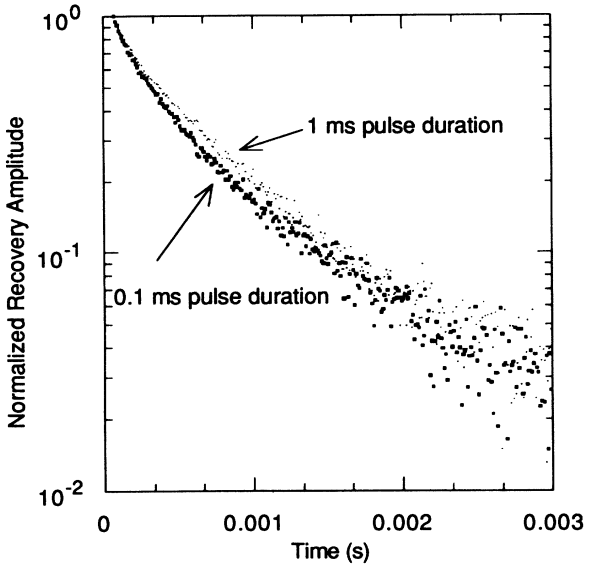

FIG. 3. Two recovery profiles for the same sample at a temperature of 4.0 K.

fourth recovery profile (0.1 ms pulses) was measured with the sample cavity enclosed in an isolation can. In this configuration, the thermal contact is provided mainly by the contact to the copper cavity bottom. Some additional thermal contact may have been provided by the low pressure of helium exchange gas. Over 3 orders of magnitude of signal amplitude, the recovery signal for the sample in the isolation can fell below the amplitude recorded for the same sample in direct contact with the helium. This behavior suggests that thermal contact for samples in the isolation can is adequate.

As is evident from the plots of the decay profiles in Fig. 2, the profiles are not perfectly exponential. The profiles display some curvature (concave up) on a semilog plot. The data in these figures can be fit to a stretched exponential. The fitting parameters for these fits are shown in Table I, and were made to a function of the form

$$y = A[\exp-(t/\tau)^{\beta}] . \quad (6)$$

There are several ways that a nonexponential form for the time dependence can be derived. One way is to assume a distribution of relaxation rates for spins at different sites in the glass. The derivation of the time dependence of a composite relaxation profile has been calculated analytically for Γ distribution of relaxation times.[25] This is a very general distribution with two adjustable parameters: the variance and the mean. The Γ distribution of relaxation times integrates to a modified Bessel function of the third kind. The lowest-order Bessel function of this kind is a stretched exponential with stretching factor $\beta=0.5$.

TABLE I. Fitting parameters for the recovery profiles in Fig. 2 to Eq. (6) of the text. The data were fit so as to minimize the rms deviation, which is listed as an indicator of the goodness of the fit. Such a fit allows large percentage deviations from the data near the tail of the recovery profiles where the amplitude is small.

Pulse duration (ms)	A	τ (s)	β	rms deviation
0.1	1.4	9.88×10^{-4}	0.56	5.04×10^{-3}
1	1.2	2.81×10^{-3}	0.66	5.72×10^{-3}
10	1.1	4.49×10^{-3}	0.68	4.59×10^{-3}
100	1.1	5.302×10^{-3}	0.64	5.79×10^{-3}

A phonon bottleneck also leads to nonexponential recoveries. If a phonon bottleneck is present, the relaxation will be governed by two coupled differential equations.[26,27] A more detailed description involving three differential equations (two for phonons, one for the spin system) has been given by Potter.[28]

Several fitting functions were tried to find an appropriate analytic form for the measured decay profiles. These included stretched exponentials, power laws, sums of two exponentials, and the sum of a stretched and an unstretched exponential. The last combination gave the lowest rms deviation in a least-squares fit to the data. Although this function fits the data very well, it has so many free parameters that is is not a useful way to characterize each decay profile. In practice, it was more enlightening to operate under experimental conditions that produced more nearly exponential recoveries, from which a rate could be determined.

Figure 3 shows a semilog plot of two recovery profiles at a temperature of 4.0 K for the same sample. By 4.0 K, the recovery profiles are more nearly exponential and pulse duration independent.

B. Lowest Yb concentration

Several pieces of each glass were examined under various experimental conditions. Data for each concentration under the most favorable experimental conditions (thin samples and short pulses) are shown in Fig. 4. The relaxation data for the lowest Yb concentration will be emphasized for two reasons. First, because it is only in the limit of very low concentration that the true spin-phonon interactions can be studied in these samples. At higher concentrations, spin-spin interactions mask the behavior of interest. Second, the temperature dependence of the Raman rate for this sample is not the usual T^9 dependence expected for Kramers' ions. Instead, the observed temperature dependence in the Raman region is approximately T^6. The relaxation data for the lowest-concentration data can be fit by a simple power law, given by

$$1/T_1 = AT + BT^n . \quad (7)$$

The values of the fitting parameters for this particular data set are $A=149\pm1$ $K^{-1}s^{-1}$, $B=0.143\pm0.009$ $K^{-n}s^{-1}$, and $n=6.08\pm0.04$. The resulting rms percentage deviation is 3.46%.

Fits to other data sets obtained for the same glass under slightly different experimental conditions gave the following results for the exponent n: 5.99 ± 0.02, 6.02 ± 0.04, and 6.31 ± 0.05, giving an average value for n of 6.1 and a standard deviation of 0.1. It should be noted that the value of the exponent n is very sensitive to mea-

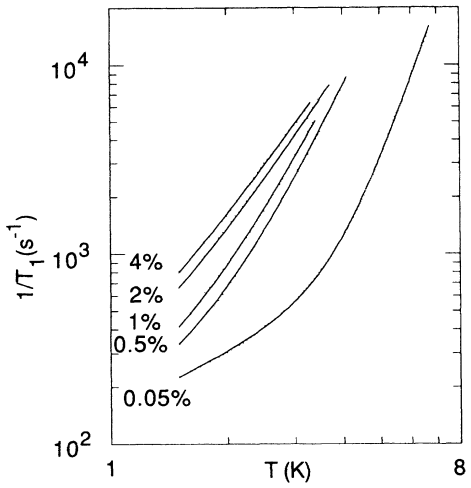

FIG. 4. Relaxation rates as a function of temperature for each Yb concentration studied. The data from the 0.05-mol % sample were fit to the sum of a direct process and a T^n Raman process [Eq. (7)]. The fits for each of the higher concentration correspond to the addition of a variable DT^n term [Eq. (13)] to the fit shown for the 0.05-mol % sample. Parameter values for the concentration dependent term are given in Table II.

surements of the fastest rates at the highest temperatures.

Transport integrals of index 8 or less reach a value that is within 0.01% of their limit for argument values of 21 or greater. Because our data were measured below 7 K, only Debye temperatures less than 147 K should be discernible as deviations from a simple power law. Thus the fit of the data to Eq. (7) with $n=6.08\pm0.04$ could be interpreted as indicating a spectral dimension of 1.54 ± 0.02 and a Debye temperature greater than 147 K. Two additional methods of reproducing the observed temperature variation of the Raman process are discussed below.

The Raman data can be fit to the standard Raman integral with an anomalously low Debye temperature, which is required to reduce the effective log-log slope from 9 to 6.08. The same data set was fit to Eq. (4) with m fixed at 3:

$$1/T_1 = AT + BT^9 J_8(\Theta/T) \ . \tag{8}$$

The resulting values of the fitting parameters were $A=160\pm1.5\ \mathrm{K}^{-1}\mathrm{s}^{-1}$, $B=(7.9\pm0.3)\times10^{-8}\ \mathrm{K}^{-9}\mathrm{s}^{-1}$, and $\Theta=40.4\pm0.5$ K, and the fit has an rms percentage deviation of 5.04%.

Values of Θ for the other data sets, previously mentioned, are $\Theta=40.2\pm0.9$, 41.2 ± 0.9, and 43 ± 1 K, yielding an average value of 41.2 K and a standard deviation of 1.1 K. The value of Θ was very sensitive to points at the end of the data set where the uncertainties in the rates were the largest.

The previous fit can be improved by making the Debye cutoff less abrupt. We consider the following form for the density of states, referring to it as an exponentially damped Debye model:

$$\rho(\nu)=\begin{cases}\nu^2 & (\nu<\nu_c)\\ \nu^2\exp[-\alpha(\nu-\nu_c)] & (\nu_c<\nu<\nu_D)\\ 0 & (\nu>\nu_D)\ .\end{cases} \tag{9}$$

This function has the Debye form for frequencies below a crossover frequency ν_c, then a more gradual cutoff, determined by a damping factor α, and equals zero for frequencies above the Debye frequency. Partitioning the frequency range in this manner was done to be consistent with theoretical predictions of a crossover frequency.[14] This improved the quality of the fit, but the optimum value of ν_c was zero.

A fit of the data was made to a transport integral of order 8 [Eq. (2)] and the density of states of Eq. (9), with $\nu_c=0$ and $\nu_{\max}$ arbitrarily large. The result was characterized by a damping factor α of $4.4\pm0.1\ \mathrm{THz}^{-1}$ and an rms percentage deviation of 3.71%. The coefficient of the associated direct relaxation rate was $A=155\pm1.1\ \mathrm{K}^{-1}\mathrm{s}^{-1}$.

Figure 5 plots the point-by-point percentage deviation of the three fits, just described, to the data shown on the lower curve of Fig. 4. All of the fits in Fig. 5 show the same general features with respect to the data, although the fit using Eq. (8) (curve 1 in Fig. 5) results in a slightly larger rms deviation than the other two.

C. Higher Yb concentrations

The fitting of data for the more concentrated samples of Fig. 4 was done using a function with a term linear in T for the direct process, a T^n Raman process, and a

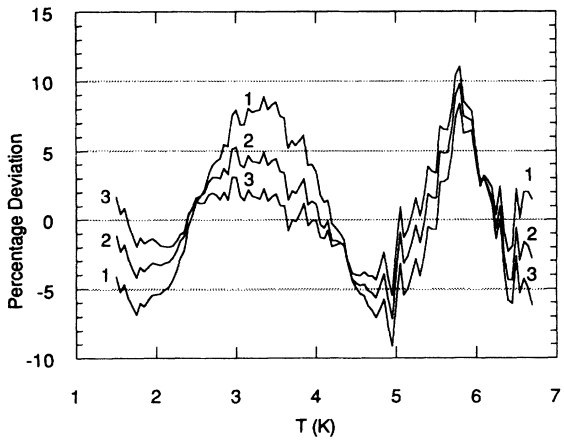

FIG. 5. Point-by-point percentage deviation of the data from each of the functions used to fit the data from the lowest Yb concentration. All three fitting functions assumed a direct relaxation rate, linear in temperature. Various functional forms for the Raman process were considered. Curve 1 includes the standard Debye density of phonon states [$\rho(\nu)\propto\nu^2$] with an upper cutoff temperature of 40.4 K [Eq. (8)]. Curve 2 includes the standard Debye density of states with an exponential damping factor [Eq. (9)]. Curve 3 uses a simple T^n power law to characterize the Raman rate [Eq. (7)]. The rms percentage deviations for curves 1, 2, and 3 were 5.04%, 3.71%, and 3.46%, respectively.

concentration-dependent term,

$$1/T_1 = AT + BT^n + (1/T_1)_c \ . \tag{10}$$

Values for A, B, and n were taken from fits to the 0.05-mol% -doped glass [Eq. (7)] and were held constant for the fits to each of the other concentrations. This method of fitting the concentration dependence has been used by Harris and Yngvesson[29] and Schulz and Jeffries.[30] The method assumes that a cross-relaxation mechanism occurs in parallel with the spin-phonon relaxation pathway. Various trial functions were used for the concentration-dependent process $(1/T_1)_c$, including the two functional forms given by Schulz and Jeffries for two limiting cases of cross relaxation between single ions and exchange-coupled pairs. The first of these trial functions is the form appropriate when the single-ion–pair relaxation is the rate-limiting step in the overall relaxation process:

$$(1/T_1)_c = D' \left[\exp\left(\frac{\Delta}{k_B T} \right) + 1 \right]^{-1} \ . \tag{11}$$

The values of Δ/k_B obtained from these fits ranged from 11.3 K for the 0.5-mol %–doped glass to 6.9 K for the 4.0-mol %–doped glass. The fit of the parameter D' to a power-law dependence in concentration is complicated by the variations in Δ. If the relaxation followed the form predicted for the single ion-pair relaxation process, the concentration dependence would be given by $D' \propto c^2$. Instead, the concentration dependence is proportional to $c^{-0.37}$. We conclude from this that the single-ion–pair relaxation process is not the rate-determining step in the overall relaxation mechanism.

A second function, predicted for the pair-bath relaxation process, appropriate when the pair-bath relaxation is the rate-limiting step in the overall relaxation process, is

$$(1/T_1)_c = D'' \mathrm{csch}(\Delta/k_B T) \ . \tag{12}$$

The value of Δ/k_B obtained for these fits ranged from 11.1 K for the 0.5-mol %–doped glass to 6.4 K for the 4.0-mol %–doped glass. Again, the fit of the parameter D'' to a power law in concentration is complicated by the wide variation in Δ. If the relaxation followed the form predicted for the pair-bath relaxation process,[30] the concentration dependence would be a simple proportionality. Instead, D'' exhibits a $c^{0.36}$ variation. The range of exchange splittings (from 6 to 12 K) derived from these fits is consistent with the values of the exchange constant measured in the trifluoride system.[30,31] However, the corresponding concentration dependence is significantly lower than the linear concentration dependence predicted by this simple theory.

A simple power law yields fits with a lower-percentage deviation than those resulting from the functions of Eqs. (11) or (12). Fits were made to a function of the following form:

$$\left[\frac{1}{T_1} \right]_c = DT^n \ . \tag{13}$$

TABLE II. Parameter values for fits of the concentration-dependent term [Eq. (13)] of the overall relaxation rate [Eq. (10)] to a power-law temperature dependence. These fits minimized the rms percentage deviation and are shown in Fig. 4.

c (mol %)	n	D ($s^{-1}K^{-n}$)	$E=D/c$ ($s^{-1}K^{-n}$)	rms % deviation
0.5	4.17	20.43	40.86	5.36
1.0	3.83	39.87	39.87	2.34
2.0	3.05	126.6	63.3	4.66
4.0	2.90	176.6	44.15	1.57

The parameter values obtained from the fit using this concentration dependence in Eq. (10) are given in Table II along with the rms percentage deviation of the fits. These fits to the experimental data are the ones shown in Fig. 4. Although the variation of D with concentration is nearly linear ($c^{1.1}$), very little can be inferred because of the range of n values.

As is apparent from the previous analysis, it is difficult to extract a meaningful concentration dependence without a specific functional form for the associated temperature variation. In Ref. 30, relaxation measurements were made on crystalline LaF_3 containing 1 at. % Yb. In fitting the data, terms corresponding to both of the limiting cases given by Eqs. (11) and (12) were used and resulted in values of $\Delta/k_B = 0.47$ and 3.9 K for the exchange splittings, respectively. Since Δ/k_B is not uniquely determined in a crystalline host, it is reasonable to expect the exchange splittings in a glass host to be randomly distributed.

IV. DISCUSSION

In fitting the Raman process in the lowest Yb concentration samples we have attempted to use functions compatible with the current theories of vibrational excitations in disordered solids. These can be characterized as conventional phonon modes, two-level tunneling states,[32,33] inherently local vibrational modes, localized phonons, and fractons (localized vibrations of a fractal structure). Reference 34 provides a general discussion of the universal characteristics of glasses, including phonon localization. Examples of the inherently local modes are bond-bending or breathing modes in isolated structural units. They are detected by Raman spectroscopy, infrared spectroscopy, and inelastic neutron scattering.[21,35] They do not transport heat nor contribute to thermal transport measurements. Localized phonons are analogues of extended acoustic phonons in crystals. The localization can result from strong scattering or fractal geometry. Experiments sensitive to these excitations include thermal transport properties, such as thermal conductivity or thermal boundary resistance, and spin-lattice relaxation measurements. The theory of Orbach *et al.*[11–17] describing localization due to fractal geometry has already been mentioned. Another description of the phenomenon of localization is localization in the Anderson sense.[36] This theory was first developed to explain electronic transport

in a random lattice. This theory has been extended to the case of phonons in a disordered elastic medium by Sompolinsky and Stephen.[37]

Experimentally, the strongest support for these models come from measurements of the thermal conductivity.[38] The mean free path l can be extracted from measurements of the thermal conductivity, and plotted as a function of the phonon energy. A localization frequency can be derived from such a plot by drawing in the line $\lambda(\omega)=l(\omega)$ and taking the intersection to be the localization edge. This is called the Ioffe-Regel localization criterion.[39] In comparing values extracted from these fits in units of temperature to other measurements made in units of frequency, we arbitrarily use the simple conversion $h\nu=k_B T$. The peak frequency in the exponentially damped cutoff model occurs at 0.45 THz. The fit [Eq. (8)] with a low Debye temperature of 40.4 K corresponds to 0.84 THz. We interpret this to mean that phonons at frequencies above roughly 1 THz are not contributing significantly to the spin-lattice relaxation process. The Ioffe-Regel localization criterion is satisfied for silicate glass at $T\approx 29$ K corresponding to $\nu=0.58$ THz. Given the approximate nature of these calculations, this numerical agreement is good.

Another experimental measurement with similarly interpreted results is the measurement of thermal boundary resistance at epoxy-metal interfaces.[40,41] Although the values for parameters describing epoxy and glass samples differ, the general aspects of the models are the same. This supports the hypothesis that the vibrational excitations in disordered solids have certain universal characteristics.

Because the spin-lattice relaxation rate is proportional to the integral over the phonon spectrum, it is not a very sensitive way to probe phonon localization. Our present analysis does not allow us to distinguish between various models for the localized modes. In particular, we cannot infer that the modes are fractons.

V. CONCLUSIONS

The dependence of the relaxation rates of Yb^{3+} spins in a host silicate glass on various experimental parameters has been explored. The experimental conditions of short pulses, low power, and thin samples provided the experimental conditions that yielded approximately exponential recoveries, independent of pulse duration and power level. Operating under these conditions allowed us to characterize the spin-lattice relaxation rate as a function of temperature for each Yb^{3+} concentration. This concentration dependence is interpreted in terms of cross relaxation to exchange-coupled pairs. No single value for the exchange energy Δ could be extracted from the fits to these data. If the fits were made to the simple form predicted for one of the limiting cases for this cross relaxation, the values of the exchange splitting obtained were in the range from 6 to 12 K. Better fits to the data were obtained using a power law.

In the glass with the lowest Yb^{3+} concentration, the effects of cross relaxation between Yb spins are minimized, and the spins provide a means of probing the low-energy vibrational excitations of the host glass. Compared with similar measurements made on crystalline material, the temperature dependence of the recovery rates for the two-phonon Raman process is anomalously weak (approximately T^6 instead of T^9). This suggests the need to modify the Debye density of states. Several models describing the vibrational density of states in a glass were presented. One feature that all of these models have in common is a critical or crossover temperature or frequency, where the vibrational excitations change in character from extended to localized. It is not possible to distinguish between the various models presented on the basis of our measurements alone. Specifically, we cannot conclude that the localized vibrational modes are fractons.

An estimate for this localization temperature or crossover temperature based on the Ioffe-Regel localization criterion can be extracted from thermal conductivity measurements in silicate glass. One of the results of this study has been to notice that a Debye temperature close to that of the localization temperature in these glasses will produce the observed T^6 temperature dependence of the Raman rate. This suggests that the relaxation mechanism is closely associated with unlocalized phonons. Exactly why this should be is not obvious, as it does not result from the usual Hamiltonian describing the spin-phonon interaction. We have used fits to the data from the lowest-concentration sample to model the phonon density of states in the glass. The models indicate that the portion of the phonon spectrum participating in the relaxation process is the low-frequency portion of the phonon spectrum.

While it is tempting to draw strong parallels between these results and similar relaxation data in frozen protein solutions, data exist from crystalline protein samples that similarly exhibit this anomalous behavior.[1] Any theory attempting to model the vibrational density of states in both the glasses and frozen protein solutions will have to account for the similar behavior exhibited by crystalline protein samples.

ACKNOWLEDGMENTS

This work was supported by the Department of Energy, Division of Materials Sciences, under Contract No. DE-AC02-76ER-01198.

*Present address: Harry Diamond Laboratories, 2800 Powder Mill Road, Adelphi, MD 20783.

[1] C. Mailer and C. P. S. Taylor, Biochim. Biophys. Acta **322**, 195 (1973).

[2] R. C. Herrick and H. J. Stapleton, J. Chem. Phys. **65**, 4778 (1976).

[3] H. J. Stapleton, J. P. Allen, C. P. Flynn, D. G. Stinson, and S. R. Kurtz, Phys. Rev. Lett. **45**, 1456 (1980).

[4] J. P. Allen, J. T. Colvin, D. G. Stinson, C. P. Flynn, and H. J. Stapleton, Biophys. J. **38**, 299 (1982).

[5]P. J. Muench, T. R. Askew, J. T. Colvin, and H. J. Stapleton, J. Chem. Phys. **81**, 63 (1984).
[6]J. T. Colvin and H. J. Stapleton, J. Chem. Phys. **82**, 4699 (1985).
[7]G. C. Wagner, J. T. Colvin, J. P. Allen, and H. J. Stapleton, J. Am. Chem. Soc. **107**, 5589 (1985).
[8]A. R. Drews, B. D. Thayer, H. J. Stapleton, G. C. Wagner, G. Giugliarelli, and S. Cannistraro, Biophys. J. **57**, 157 (1990).
[9]J. P. Gayda, P. Bertrand, A. Deville, C. More, G. Roger, J. F. Gibson, and R. Cammack, Biochem. Biophys. Acta **581**, 15 (1979).
[10]C. P. Scholes, R. Janakiraman, H. Taylor, and T. E. King, Biophys. J. **45**, 1027 (1984).
[11]S. Alexander, C. Laermans, R. Orbach, and H. M. Rosenberg, Phys. Rev. B **28**, 4615 (1983).
[12]O. Entin-Wohlman, S. Alexander, R. Orbach, and Kin-Wah Yu, Phys. Rev. B **29**, 4588 (1984).
[13]B. Derrida, R. Orbach, and Kin-Wah Yu, Phys. Rev. B **29**, 6645 (1984).
[14]A. Aharony, S. Alexander, O. Entin-Wohlman, and R. Orbach, Phys. Rev. B **31**, 2565 (1985).
[15]S. Alexander, O. Entin-Wohlman, and R. Orbach, Phys. Rev. B **32**, 6447 (1985).
[16]S. Alexander, O. Entin-Wohlman, and R. Orbach, Phys. Rev. B **33**, 3935 (1986).
[17]S. Alexander, O. Entin-Wohlman, and R. Orbach, Phys. Rev. B **35**, 1166 (1987).
[18]M. Weber, J. Lynch, H. Blackburn, and D. Cronin, IEEE J. Quantum Electron. **QE-19**, 1600 (1983).
[19]C. C. Robinson and J. T. Fourier, J. Phys. Chem. Solids **31**, 895 (1970).
[20]O. L. Anderson, J. Phys. Chem. Solids **12**, 41 (1959).
[21]U. Buchenau, M. Prager, N. Nucker, A. J. Dianoux, N. Ahmed, and W. A. Phillips, Phys. Rev. B **34**, 5665 (1986).
[22]R. V. Pound, Rev. Sci. Instrum. **17**, 490 (1946).
[23]A. C. Anderson, in *Nonequilibrium Superconductivity, Phonons, and Kaptiza Boundaries*, edited by Kenneth E. Gray (Plenum, New York, 1981).
[24]D. L. Smith and H. J. Stapleton, Phys. Rev. B **33**, 7417 (1986).
[25]A. Aharoni, J. Appl. Phys. **57**, 4702 (1985).
[26]P. L. Scott and C. D. Jeffries, Phys. Rev. **127**, 32 (1962).
[27]B. W. Faughnan and M. W. P. Strandberg, J. Phys. Chem. Solids **19**, 155 (1961).
[28]W. H. Potter, Phys. Rev. B **5**, 1178 (1972).
[29]E. A. Harris and K. S. Yngvesson, J. Phys. C **1**, 990 (1968).
[30]M. B. Schulz and C. D. Jeffries, Phys. Rev. **149**, 270 (1966).
[31]S. Kern and P. M. Raccah, J. Phys. Chem. Solids **26**, 1625 (1965).
[32]P. W. Anderson, B. I. Halperin, and C. M. Varma, Philos. Mag. **25**, 1 (1972).
[33]W. A. Phillips, J. Low Temp. Phys. **7**, 351 (1972).
[34]J. E. Graebner, B. Golding, and L. C. Allen, Phys. Rev. B **34**, 5696 (1986).
[35]J. M. Carpenter and D. L. Price, Phys. Rev. Lett. **54**, 441 (1985).
[36]P. W. Anderson, Phys. Rev. **109**, 1492 (1958).
[37]S. J. Sompolinsky and M. J. Stephen, Phys. Rev. B **27**, 5592 (1983).
[38]R. C. Zeller and R. O. Pohl, Phys. Rev. B **4**, 2029 (1971).
[39]A. F. Ioffe and A. R. Regel, Prog. Semicond. **4**, 237 (1960).
[40]D. S. Matsumo, C. L. Reynolds, Jr., and A. C. Anderson, Phys. Rev. B **16**, 3303 (1977).
[41]C. L. Reynolds, Jr., and A. C. Anderson, J. Low Temp. Phys. **21**, 641 (1975).